



Hydrogen Storage in VN_x-H_y Thin Films

Viktor Bryk¹, Aleksey Guglya^{1*}, Aleksandr Kalchenko¹, Ivan Marchenko¹, Yuriy Marchenko¹, Elena Solopikhina (Melnikova)¹, Victor Vlasov¹, Evgeniy Zubarev²

¹National Science Center “Kharkov Institute of Physics and Technology”, Kharkov, Ukraine

²National Technical University “Kharkov Polytechnic Institute”, Kharkov, Ukraine

Email: *guglya@kipt.kharkov.ua

Received 22 November 2015; accepted 9 December 2015; published 14 December 2015

Copyright © 2015 by authors and OALib.

This work is licensed under the Creative Commons Attribution International License (CC BY).

<http://creativecommons.org/licenses/by/4.0/>



Open Access

Abstract

Vanadium or its alloy-based hydrides are intensively studied at the moment with regard to their use as hydrogen absorbents. Most experiments were carried out using “bulk” materials. This paper uses ion beam-assisted deposition technology (IBAD) to create thin-film nanocrystalline VN_x-H_y hydrogen storages. The transmission electron microscopy and scanning electron microscopy were used to study the initial stages of the film formation. The main mechanisms of the formation of intergranular pores in nanogranular structures have been established. The interrelation of the parameters of the IBAD and those of film structure has been shown. The obtained data allowed for the explanation of the mechanisms of hydrogen absorption and desorption by thin films. It was shown that the availability of branched network of intergranular pores allows VN_x-H_y structures to accumulate hydrogen within a few minutes at a pressure of 0.5 MPa. Hydrogen in amount of up to 2.55 wt% is retained in the films of 3 μm thick at room temperature and atmospheric pressure. The hydrogen desorption starts at 100°C.

Keywords

Nanocrystalline Structures, Hydrogen, Absorption, Storage, Thin Films, Ion-Beam Assisted Deposition

Subject Areas: Nanometer Materials

1. Introduction

To develop hydrogen storages for fuel elements we use compact and light materials that have a high hydrogen capacity. Therefore, single-component and complex hydrides based on light metals (Mg, Ca, Na, Al, Be) are of great interest for us not only because of their tendency to store hydrogen in large amounts but also because of substantial weight fraction of hydrogen in hydrides of these metals.

*Corresponding author.

In addition, hydrides based on relatively light transient metal, in particular vanadium, can also be used as hydrogen storages. Vanadium has a low hydrogen desorption temperature of 40°C, and the gravimetric capacity is 2.1 wt%, which is comparable with the capacity of porous carbon and metal-organic structures [1] [2]. It should also be noted that the amount of absorbed hydrogen atoms per unit volume in VH_2 is much higher in comparison, for example, with MgH_2 [3]. And finally, vanadium as a catalyst noticeably improves thermodynamics and kinetics of hydrogen absorption by single-component and complex hydrides [4] [5]. Particularly the above facts can explain a heightened interest to vanadium [6]-[9]. The obtained results prove that it can be used for the hydrogen storage.

All the above research was done using the “bulk” materials. Unfortunately, bulk metal hydrides have many drawbacks, in particular the decelerated diffusion of hydrogen deep into the material, and accordingly, low depth of hydrogen saturation zone, and a low heat transmission from the surface deep into the specimen. These drawbacks produce adverse effect on thermodynamic and kinetic characteristics of these hydrides. In addition, massive specimens require the application of thin films onto them that would protect the metal hydride from the oxidation or speed up the dissociation of hydrogen molecules on their surfaces [10]-[13].

Therefore, in addition to “bulk” hydrides thin-film structures, in particular Mg [14]-[18], V [19]-[21], Ti [22] [23], Nb [24] [25], Pd [26] [27], Mg/Pd [28] [29], Mg/Ni [30] have been studied intensively. Thin films have definite advantages in comparison with “bulk” specimens, in particular a high surface area-to-volume material ratio facilitates the hydrogen formation kinetics; a zero temperature gradient along the film thickness provides accelerated hydrogen diffusion; a variety of the methods used for the deposition of thin films allows for the production and study of polycrystalline, fine-crystalline, nanocrystalline single and multicomponent structures and protective and catalytic coatings can easily be applied after the deposition of the main material. The use of different test methods allows for the complex analysis of structural changes that occur in the films during absorption and desorption of hydrogen by them.

In particular, it was revealed that a change in electrical resistance of Mg and V during the absorption of hydrogen by them is directly related to the amount of absorbed molecules [14] [19] [20] [24]. While studying the relationship of the electrical resistance of Pd films as a function of their thickness the authors of the paper [27] noticed the emergence of the hysteresis loop during the hydrogen absorption and/or desorption process. The analysis of the hysteresis loop allows us to determine how the film thickness affects α -phase-to- β -phase transition kinetics. The studies of electrophysical characteristics also allow for the determination of the most optimal parameters of hydrogen absorption by Mg films [31], and also the efficiency of the influence of protective Pd coatings on the hydrogen absorption kinetics [28].

The studies of film structures and their surfaces using the transmission electron microscopy, scanning microscopy and X-ray analysis showed a considerable increase (up to 20%) in the grain size [16] [26], and in the material volume during the hydrogen absorption [17] [32] [33]. In addition it was shown that the transition to the nanocrystalline structure of the films results in the cardinal improvement of the kinetics of hydrogen absorption by them [21] [22] [26]. The transmission electron microscopy also allows us to investigate the formation of the hydride phase at the nucleation stage [17]. The origination of strong compressive stresses in different metal films (Ti, Mg/Pd, Pd/Nb) during their saturation with hydrogen has been established [21] [33] [34].

The analysis of the above material shows that the use of contemporary non-equilibrium methods used for the deposition of thin films allows us to shape structures capable of storing hydrogen in amount exceeding 6 wt% [21]. In order to obtain such a result with regard to vanadium films it is necessary to increase thermodynamic stability of the “loose” hydride VH_2 through the transition to a closer-packed structure, for example, that of complex nitrogen-containing hydride. To improve hydrogen adsorption kinetics we need to form nanostructure with a minimum grain size and maximally developed boundary system. To improve gravimetric characteristics it is necessary to create such a nanocrystalline structure, which would be able to accumulate hydrogen not only in atomic state (hydrides), but also in molecular state (pores).

In this paper the main attention was paid to the establishment of the interconnection between the structure of the thin-film complex hydride $\text{VN}_x\text{-H}_y$ and its absorption characteristics. Using the transmission electron microscopy and scanning microscopy we studied the process of the formation of nanocrystalline VN_x structure starting from the stage of its nucleation until the thickness of 3 μm is reached. The interconnection between the hydrogen storage and/or release kinetics in thin films $\text{VN}_x\text{-H}_y$ and the change of their structure has been studied.

2. Experimental Methods

The research done by us earlier showed (see, for example, [35]) that the IBAD method can be used to obtain both compact and porous nanocrystalline thin-film structures. This method provides the deposition of thin-films under the bombardment with gas ions, whose energy reaches 50 keV. In comparison with plasma techniques a specific distinctive feature of this method is that the evaporation process of the metal component is functionally separated from the ion stimulated bombardment with high-energy gas ions. This special feature allows us to regulate any process parameters independently of each other, changing thus the structure and properties of composite materials in a broad range.

Nanocrystalline thin VN_x films described in this paper were obtained through the evaporation of vanadium from electron-beam crucible. The deposited condensate was irradiated with the ion mixture of $\text{N}^+ + \text{N}_2^+$ and He^+ in equal fractions, the ion energy was 30 keV. The ion flow-to-atom flow ratio was equal to 0.4 ion/atom; the substrate temperature was $< 50^\circ\text{C}$. The metals were deposited onto the KCl substrate coated with the carbon film. To study the initial stage of the formation we used the technique that allows us to mask in turn some substrate section after definite time intervals [36]. We obtained some films of 3 to 100 nm and 3 μm thick whose structure was studied using the transmission electron microscope JEM 100C and scanning microscope JSM7001F. The films of 3 μm thick were simultaneously deposited onto sapphire substrates of 0.5 mm thick with the area of 1.5×1.5 cm. These objects were used to study gas release spectra. The films were saturated with hydrogen at room temperature and a pressure of 0.5 MPa during one hour.

To measure the full amount of the absorbed hydrogen, saturated by hydrogen specimens were placed into the vacuum chamber, which was preliminarily evacuated to a pressure not worse than 10^{-3} Pa. The amount of hydrogen released during the annealing was determined in terms of a change in the pressure in the closed chamber, which was controlled using the vacuum sensor. While studying the hydrogen thermodesorption spectra the valve was opened and the chamber was connected to the turbomolecular pump and mass-spectrometer. Consideration was given to two types of gas-release spectra. The peak value of the thermodesorption of molecular hydrogen was measured after every 10 degrees. The total spectrum of thermodesorption was recorded after each 50 degrees in the mass interval of 1 to 32.

3. Results

3.1. The Initial Stage of Thin Film Formation

The process of IBAD method of the vanadium film occurs during the bombardment of the condensed material with N^+ , N_2^+ and He^+ ions. The voltage on the accelerating tube is equal to 30 kV. N^+ and He^+ ions have energy of 30 keV and N_2^+ ions have energy of 15 keV. The ranges of ions whose mass and energy considerably differ will be different. Under such conditions the defects are distributed inhomogeneously in the depth of the formed film at the initial stage of the film deposition (the film thickness is less than the value of helium ion range) [17]. Therefore, the film structure at the depths higher and/or lower than the value of helium ion range will be different.

For the quantitative assessment of the conditions under which the film structure and its phase composition are formed we carried out the mathematical simulation of the defect formation (**Figure 1(a)**) and the implantation of nitrogen and helium atoms (**Figure 1(b)**) into the vanadium film, deposited under the irradiation, using the SPURT program and the technique described by us earlier [37]. As the film thickness is increased the deposited material is exposed to the action of continuously increasing flow of radiation defects and that of the amount of implanted ions. The influence of nitrogen ions on the structure and composition of the vanadium film is terminated at the depth of 80 nm. The level of damages at thicknesses exceeding 80 nm is slightly increased and it happens solely due to the influence of helium ions. The amount of implanted nitrogen at such thicknesses is not changing any longer and the helium concentration is increased almost ten times. The influence of helium ions on the formed film structure is terminated at the depth of 250 nm (it is not shown in the Figure). Thus, the computations show that the thickness of the near-surface not formed zone is within 250 nm. Therefore, it cannot produce a distinct influence on gravimetric characteristics of the films of 3 μm thick. A total estimated content of nitrogen and helium implanted into the film of >250 nm thick is within 12 at%.

In order to study the film structure at the main stages of its formation we used the method of the sequential masking of the individual sections of the film as it was deposited. **Figures 2(a)-(f)** show the photos of VN_x

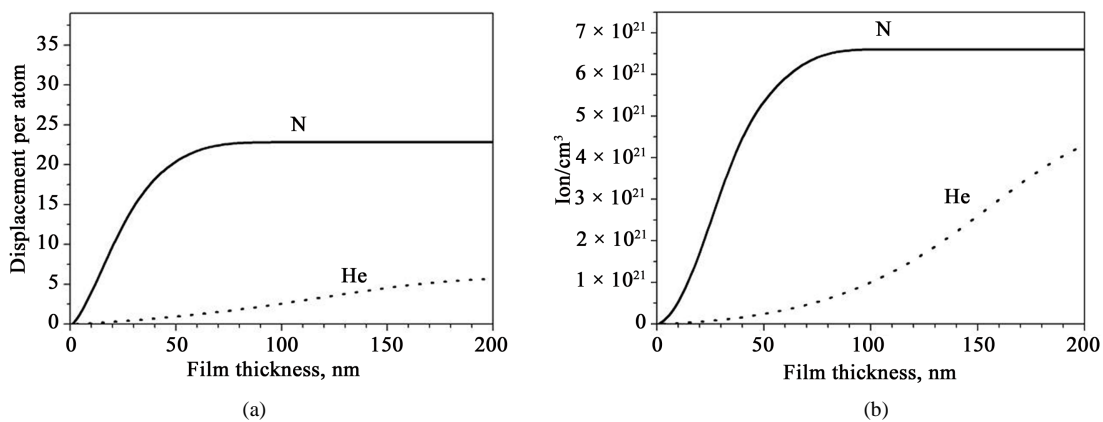
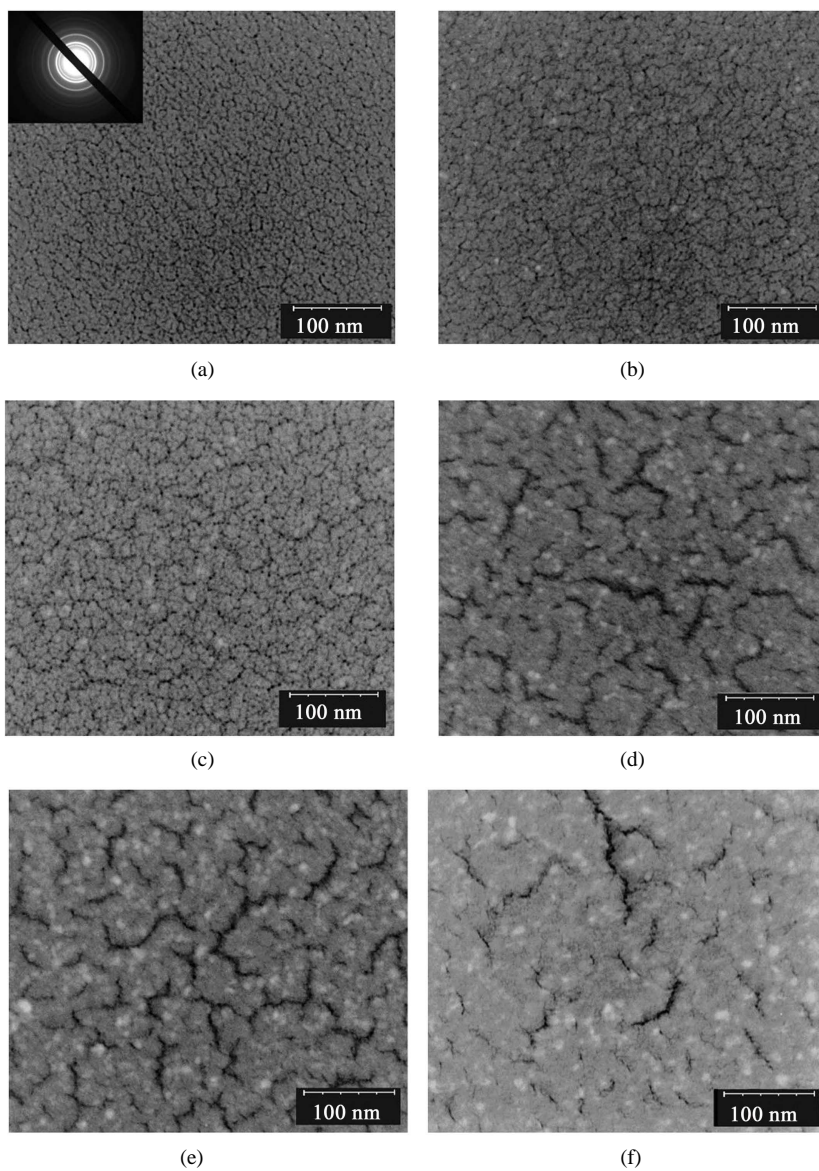


Figure 1. Damages distribution pattern (displacement per atom) (a) and implanted nitrogen and helium atoms (b) in the VN_x film. The ion flow-to-vanadium and titanium atom flow ratio is 0.4 ion/atom.



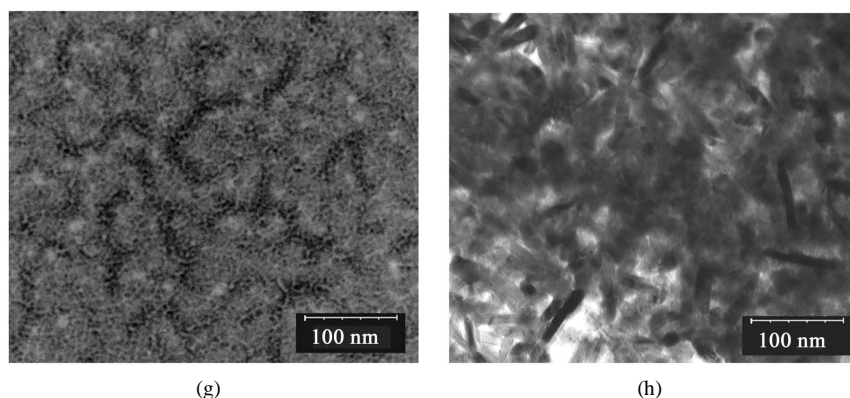


Figure 2. Electron-microscopy images of the structure of VN_x films at different deposition stages. The given film thicknesses except those in (h) are all estimated values. (a) 3 nm; (b) 6 nm; (c) 10 nm; (d) 14 nm; (e) 20 nm; (f) 25 nm; (g) 40 nm; (h) 3000 nm.

condensates whose thickness varies in the range of 3 to 25 nm. (The Figure shows reversed images for the visualization). **Figure 2(h)** shows the electron microscopy image of the formed structure (3 μm thick). It can be seen that the formation of the solid film is terminated at a thickness of 3 nm. The condensate has the nanocrystalline structure. The average grain size is 5 to 8 nm, and the density is $>10^{12} \text{ cm}^{-2}$. The grains are arranged to form one layer. The boundary width is <1 nm. The pores of 3 to 5 nm are present actually in all triple and fourfold intergranular joints. In the film of 10 nm thick the grains are united into the blocks separated by wider boundaries between them. Starting from a thickness of 10 nm these boundaries are extended and turn into specific ruptures of ~ 100 nm long and $\sim 2 - 3$ nm wide.

The film ruptures are visible until the film of ~ 25 nm is formed. Any changes in the distribution of grains in the space between the ruptures have not been observed, **Figure 2(g)**. (The image in **Figure 2(g)** is similar to that in **Figure 2(e)**, though it was taken at different focusing conditions). Their average size is equal to 5 - 8 nm. It is rather difficult to visualize the ruptures at the film thickness of $>30 - 40$ nm, when the formation of the second grain layer is finished. The studies performed at the initial stage of the formation of the structure of VN_x films showed that these films consist of subgrains of 5 to 8 nm that are grouped in their turn into larger items, *i.e.* the grains of 70 to 100 nm. The boundary thickness between the subgrains is <1 nm.

To determine the finite structure of the films we prepared the objects from condensates of 3 μm thick for the electron microscopy studies. **Figure 2(h)** shows that the finite structure of VN_x film consists of grains of 70 to 100 nm separated from each other by open broad canals. The crystalline structure of the films at all stages of their deposition corresponds to the fcc structure of vanadium nitride.

3.2. Absorption/Desorption Processes

During the hydrogen absorption and desorption of $\text{VN}_x\text{-H}_y$ films we carried out the electron microscopy studies of structural and phase changes in this material. **Figure 3** gives the data of the transmission (a, b, c) and scanning (d, e, f) electron microscopy of $\text{VN}_x\text{-H}_y$ films in their initial state (a, d), after the hydrogen uptaking (b, e) and hydrogen desorption (c, f). The film thickness is 3 μm .

It is seen that in their original state the films consist of disordered non-equiaxial grains. The grains have cylindrical shape whose length is equal to 50 - 70 nm and the bottom diameter is 10 to 15 nm. Due to the fact that the grains are arranged chaotically the major portion of the film has pores of arbitrary shape. It is impossible to measure their size and form.

Hydrogen-saturated films acquire a round shape and their diameter varies in the range of 30 to 100 nm (**Figure 3(e)**). After the hydrogen desorption, the size and shape of the grains are very close to those they had in their initial state. However, it is not excluded that some grains merge forming larger objects of irregular shape. The micro diffraction analysis initial and uptaking films showed no other phases but the fcc structure of vanadium nitride. The quantitative microanalysis showed that the content of nitrogen in the original film and in the film after the gas release remains unchangeable, *i.e.* < 3 at%. Helium was not found.

The results of desorption investigations are shown in **Figure 4**. **Figure 4(a)** gives the released hydrogen

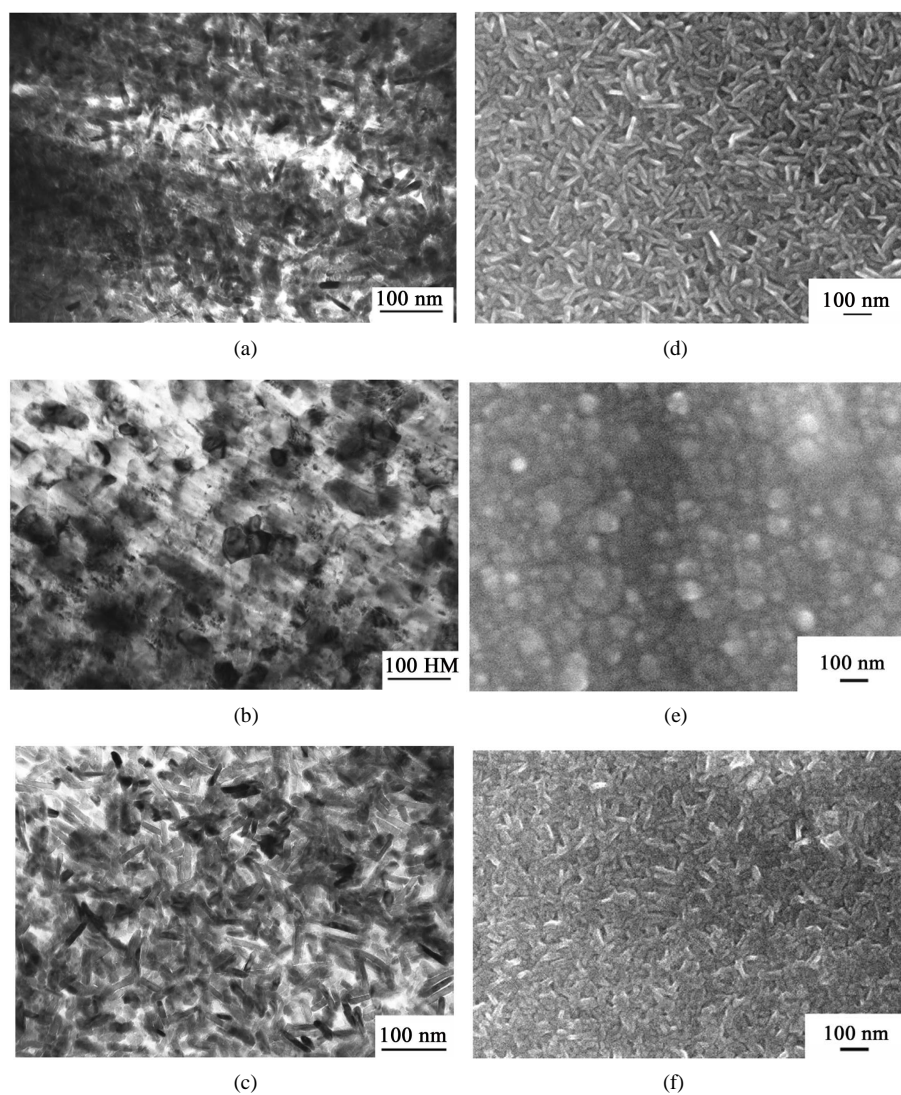


Figure 3. The structure of $\text{VN}_x\text{-H}_v$ films: (a), (d) is the original state, (b), (e) are the hydrogen-stored films and (c), (f) are the annealed films.

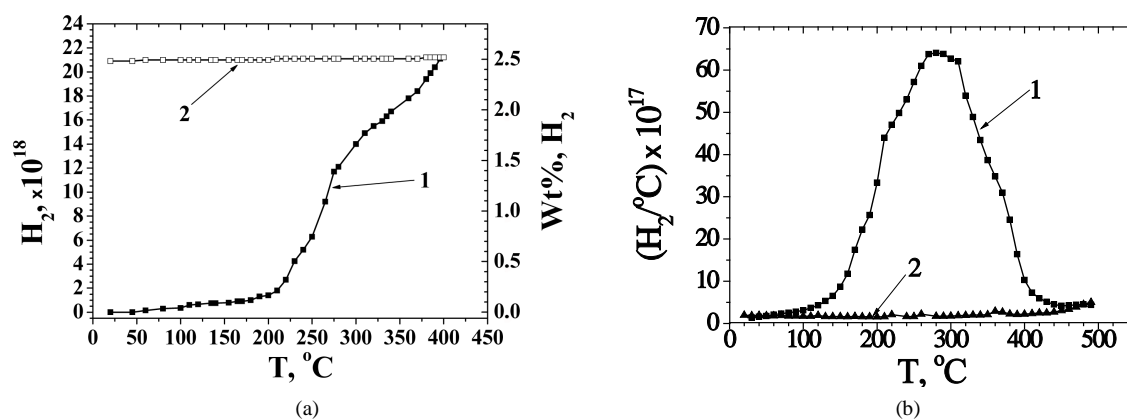


Figure 4. (a) the relationship of a change in the amount of hydrogen in the annealing chamber during heating and cooling of the $\text{VN}_x\text{-H}_v$ film. 1—heating, 2—cooling; (b) Hydrogen thermodesorption spectra of $\text{VN}_x\text{-H}_v$ film. 1—first heating, 2—second heating.

amount as a function annealing temperature. It is seen that the hydrogen desorption starts already at 80°C. At 250°C the number of the molecules of the desorbed hydrogen reaches 6×10^{18} H₂ (0.72 wt%). On reaching 400°C a total mass of the released hydrogen exceeds 2.55 wt%. While cooling the specimen a slight decrease in pressure inside the working chamber is observed, which is indicative of that the portion of released hydrogen is readsorbed by the VN_x-H_y film. Total decrease in pressure inside the chamber during cooling to 20°C corresponds to the absorption of 0.3×10^{18} hydrogen molecules, which corresponds to 0.04 wt% H₂.

Figure 4(b) gives the appropriate spectrum of thermodesorption. It is seen that hydrogen starts releasing already at 100°C. A maximum desorption rate is observed in the temperature range of 200°C - 275°C. The analysis of thermodesorption spectra that were measured after each 50 degrees showed no emergence of new peaks and no increase in the peak amplitude that was recorded at 20°C (H₂O, NH₃, N₂, O₂).

4. Discussion of the Results

The analysis of the curves in **Figure 1** shows that a total estimated content of nitrogen implanted into the film of >80 nm thick is approximately equal to 12 at%. In the thinnest films of 5 to 10 nm thick content of nitrogen is within 0.1 at%. At such concentrations the formation of vanadium nitride can hardly be expected. Nevertheless, the micro diffraction patterns of all the films show the reflection of vanadium nitride from the planes of the fcc structure. On the other part the microanalysis data show that the amount of hydrogen in the formed film of 3 μm thick makes up 2 to 3 at%. It is evident that the emergence of vanadium nitride phase in thin films and low nitrogen content in thick specimens cannot be explained just by the implantation of nitrogen ions into the film lattice using the ion beam.

The vanadium deposition under the ion stimulated irradiation when the ion source is operated can occur at a total nitrogen and helium pressure in the working chamber of 4×10^{-3} Pa. In addition, the deposition of vanadium vapors is accompanied by the continuous adsorption of nitrogen molecules and helium atoms by the substrate surface. Moreover, in such vacuum the adsorption rate does not yield to that of vanadium condensation rate. The dissociation of nitrogen molecules occurs in the ion bombardment environment. Taking into consideration the fact that the Gibbs free energy of the formation of vanadium nitride is rather low [38] the substrate surfaces will experience a continuous chemisorption of nitrogen atoms and the formation of vanadium nitride. Particularly this fact can explain the formation of vanadium nitride at the earliest stages of the film growth.

The formation of nitride phase is accompanied by the physical adsorption of nitrogen molecules and helium atoms, which results in the inhibition of diffusion processes on the film surface. As a result the mass nucleation of fine grains occurs. These are slightly oriented relatively each other and their boundaries have been saturated with nitrogen molecules and helium atoms. The radiation-assisted diffusion of adsorbed gas atoms and those implanted during the radiation stimulates the continuous inflow of gas molecules and atoms to the grain boundaries. At a certain stage of the film growth the amount of gas admixtures at grain boundaries and in the domain of triple intergranular joints becomes sufficient for the disruption of boundaries and formation of ruptures of 50 to 100 nm long (**Figures 2(d)-(f)**). This size is very close to the size of grains registered by the scanning microscope (**Figure 3(d)**). It is evident that the formation of chaotically arranged cylindrical grains results from the formation of such ruptures. During the film deposition nitrogen and helium ions penetrate to a depth, which significantly exceeds the diameter (10 to 15 nm) of the formed grains. These gas admixtures are not kept by the film and escape through the formed ruptures. Such a process retains the ruptures between the grains and provides the formation of cylindrically shaped grains surrounded by the pores.

Helium has not been found in the films. Taking into consideration a high mobility of helium vacancy clusters [39] one can assume that during the film formation helium migrates to its surface and it is desorbed by it. Helium is released due to the rupture formation and also during its diffusion across the grain boundaries.

Nitrogen concentration in the formed VN_x structure is much lower in comparison with the estimated one. It is known that during the polycrystalline-to-nanocrystalline structure transition the surface fraction of the grain in which the equilibrium concentration of vacancies differs from that in the “bulk” sample is increased. The equilibrium concentration of vacancies in the grain on the whole is also increased, accordingly [40].

$$C_s = C_v \exp(-\Delta E_s/kT) \quad (1)$$

where ΔE_s is the difference in the energies of the formation of vacancies in a small particle and also in a bulk specimen. In addition Frenkel [41] showed that ΔE_s depends on the surface energy of a small particle “ σ ” and its size “ r ” in the following way

$$\Delta E_s = -3\sigma\Omega/r \quad (2)$$

where Ω is the atomic volume.

Therefore, the concentration of vacancies in the particle of a small size depends on the particle size in the following way

$$C_s = C_v \exp(3\sigma\Omega/rkT) \quad (3)$$

It follows from the expression (3) that the equilibrium concentration of vacancies in the particles of a small size can significantly exceed that in “bulk” specimens. The analogous relationship is also available for the diffusion coefficient [40].

In the two-component structure, which is peculiar for vanadium nitride, an increase in the equilibrium concentration in the subgrains can occur exclusively due to nitrogen atoms. As a result the stoichiometric compound $\text{VN}_{1.0}$ exists only in the central region of grains. Grain boundaries have actually no nitrogen. Taking into consideration this explanation we can understand the reasons for rather low content of nitrogen in VN_x films, in particular 2 - 3 at%.

In the case of physical adsorption of hydrogen by these structures we suppose that intergranular boundaries and pores are quickly filled with gas. Further, as the pressure in pores is increased the partial dissociation of hydrogen molecules and the diffusion of atomic hydrogen inside them occur (Figure 5). The intergrain channels are short and broad. In such a situation after the hydrogen-saturated film is removed from the chamber the portion of hydrogen, which was kept by intergrain channels, will leave the film. Therefore, the main hydrogen traps in $\text{VN}_x\text{-H}_y$ films are subgrains (5 to 8 nm) and the pores between them (3 to 5 nm) (Figure 5(d)). The space between the large grains remains unfilled with hydrogen.

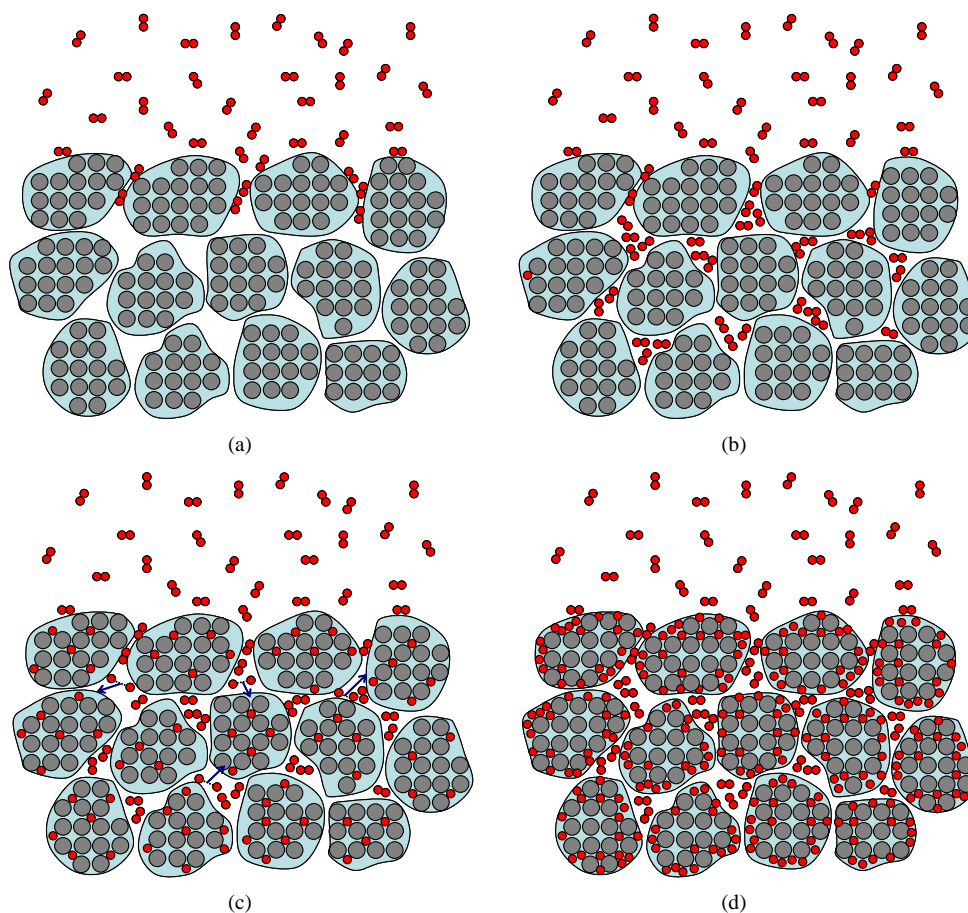


Figure 5. The diagram of hydrogen storage by sub-grains $\text{VN}_x\text{-H}_y$ films. Only one grain is shown. (a) Adsorption & diffusion; (b) Adsorption & diffusion; (c) Hydrogen dissociation; (d) Vacancy traps filling.

Instead the BET method the procedure proposed in [42] was used to determine the film material porosity. The elemental composition and the film thickness in units of “the number of arbitrary atoms $\times \text{cm}^{-2}$ ” were determined using the data of Rutherford 1.8 MeV He^+ ion backscattering spectrometry. In our case, the film thickness D was $2290 \times 10^{15} \text{ arb.at}\cdot\text{cm}^{-2}$. The thickness d of the same film measured using a profilometer was $3 \times 10^{-5} \text{ cm}$. To calculate the film density, the following formula was used [42]: $\rho = DA/d$, where A is the mass of the arbitrary film atoms in grams and d is the film thickness. In our case, the mass of the arbitrary film atoms was $51.5 \times 10^{-24} \text{ g}$. According to the formula, we hence find that the film material density is $3.9 \text{ g}\cdot\text{cm}^{-3}$. Correlating the calculated density with the density of vanadium nitrides containing in the film composition ($6.1 \text{ g}\cdot\text{cm}^{-3}$), we found that the film material porosity was $36\% \pm 3\%$.

The data of selected-area electron-diffraction analysis showed no emergence of the hydride phase. Therefore, the most probable traps for hydrogen atoms can be vacant positions in the VN_x lattice. It was shown above that the presence of 2 - 3 at% nitrogen in nitride is indicative of a high equilibrium concentration of vacant sites in the positions that should be occupied by nitrogen atoms. These sites are efficient traps for hydrogen atoms. Using the TiC_x compound as an example it was shown that the higher the degree of deviation from the stoichiometry ($x < 0.6$), the higher the number of hydrogen atoms that can be accumulated inside the crystal lattice [43] [44]. Each vacancy can retain up to 4 hydrogen atoms. The creation of the hydride phase is energetically less advantageous. Therefore, we believe that vacant positions in the surface regions of subgrains are most likely the sites for the adsorption of hydrogen atoms.

The configuration of intermediate subgrain pores in our film structures is not just a system of pores that directly traverse each other (it is peculiar for metal-&-organic and carbon film structures). In our case the pores are interconnected by relatively long ($\sim 10 \text{ nm}$) intermediate subgrain boundaries, whose width does not exceed 1 nm. This value is very closely related to the most optimal (0.6 nm) design size at which hydrogen will be retained in its molecular state [45]. The availability of such branched pore system connected by narrow and long channels provides fast delivery of molecular hydrogen to the film volume and its retention at room temperature.

5. Conclusions

The results given in this paper show that the use of IBA allows not only for the controlled formation of nanoporosity with prescribed parameters but also for the embedment of this nanoporosity into the nanocrystalline structure of a matrix. The material produced in such a way is capable of accumulating hydrogen at low pressures and room temperature. The availability of broad channels between the grains provides high diffusion mobility, which allows hydrogen to accumulate and release from the material within a short period of time. The studies of the initial stage of the deposition of VN_x films allowed for the establishment of the mechanism of the formation of the grains of a cylindrical shape and intergranular nanopores. The subgrain structure formed inside the grains stores hydrogen in two types of traps, in particular in subgrain pores and vacancies inside $\text{VN}_x\text{-H}_y$ subgrains.

Varying the basic parameters of the IBA process and first of all its radiation component it is possible to produce nanocrystalline porous structures in which the grain size can be both higher and lower than the pore diameter. Just the appropriate relationship between the sizes of these elements of the crystalline structure will allow for the fabrication of solid-state hydrogen storages with suitable characteristics.

The analysis of thermodesorption curves showed that helium implanted during the film deposition is not kept inside the pores and it does not prevent the storage of hydrogen by them. During the hydrogen absorption nitrogen is not interacting with helium and it forms no stable compounds (for example, NH_3). The fcc structure of vanadium nitride is stable during its heating and hydrogen absorption. During annealing of hydrogen-saturated films the marked release of other gas admixtures in addition to hydrogen has not been revealed.

References

- [1] Hirscher, M., Panella, B. and Schmitz B. (2010) Metal-Organic Frameworks for Hydrogen Storage. *Microporous and Mesoporous Materials*, **129**, 335-339. <http://dx.doi.org/10.1016/j.micromeso.2009.06.005>
- [2] Züttel, A., Sudan, P., Mauron, Ph., Kiyobaiashi, T., Emmenegger, Ch. and Schlappbach, L. (2002) Hydrogen Storage in Carbon Nanostructures. *International Journal of Hydrogen Energy*, **27**, 203-212. [http://dx.doi.org/10.1016/S0360-3199\(01\)00108-2](http://dx.doi.org/10.1016/S0360-3199(01)00108-2)
- [3] Niemann, M., Srinivasan, S., Phani, A., Kumar, A., Goswami, D.Y. and Stefanakos, E.K. (2008) Nanomaterials for Hydrogen Storage Applications: A Review. *Journal of Nanomaterials*, **2008**, Article ID: 950967. <http://dx.doi.org/10.1155/2008/950967>

- [4] Liang, G., Huot, J., Boily, S. Neste, A.V. and Schulz, R. (1999) Hydrogen Storage Properties of the Mechanically Milled $\text{MgH}_2\text{-V}$ Nanocomposite. *Journal of Alloys and Compounds*, **291**, 295-299. [http://dx.doi.org/10.1016/S0925-8388\(99\)00268-6](http://dx.doi.org/10.1016/S0925-8388(99)00268-6)
- [5] Yu, X., Wu, Z., Chen, Q., Dou, T., Chen, J., Xia, B. and Xu, B. (2007) Effect of V Addition on Activation Performances $\text{TiMn}_{1.25}\text{Cr}_{0.25}$ Hydrogen Storage Alloy. *Journal of Materials Processing Technology*, **182**, 549-554. <http://dx.doi.org/10.1016/j.jmatprotec.2006.09.016>
- [6] Orimo, S., Kimmerle, F. and Majer., G. (2001) Hydrogen in Nanosructured Vanadium-Hydrogen Systems. *Physical Review B*, **63**, Article ID: 094307. <http://dx.doi.org/10.1103/PhysRevB.63.094307>
- [7] Yukawa, H., Takagi, M., Teshima, A. and Morinaga, M. (2002) Alloying Effects on the Stability of Vanadium Hydrides. *Journal of Alloys and Compounds*, **330-332**, 105-109. [http://dx.doi.org/10.1016/S0925-8388\(01\)01526-2](http://dx.doi.org/10.1016/S0925-8388(01)01526-2)
- [8] Planté, D., Raufast, C., Miraglia, S., Rango, P. and Fruchart, D. (2013) Improvement of Hydrogen Sorption Properties of Compounds Based on Vanadium “bcc” Alloys by Mean of Intergranular Phase Development. *Journal of Alloys and Compounds*, **580**, S192-S196. <http://dx.doi.org/10.1016/j.jallcom.2013.03.080>
- [9] Seo, Ch.Y., Kim, J.H., Lee, P.S. and Lee, J.-Y. (2003) Hydrogen Storage Properties of Vanadium-Based b.c.c. Solid Solution Metal Hydrides. *Journal of Alloys and Compounds*, **348**, 252-257. [http://dx.doi.org/10.1016/S0925-8388\(02\)00831-9](http://dx.doi.org/10.1016/S0925-8388(02)00831-9)
- [10] Pick, M. and Greene, M. (1980) Uptake Rates for Hydrogen by Niobium and Tantalum: Effect of Thin Metallic Overlayers. *Journal of the Less Common Metals*, **73**, 89-85. [http://dx.doi.org/10.1016/0022-5088\(80\)90346-X](http://dx.doi.org/10.1016/0022-5088(80)90346-X)
- [11] Nakamura, K. (1981) Hydrogen Absorption Kinetics of Niobium with an Ionplated Nickel Overlayer. *Journal of the Less-Common Metals*, **80**, 65-80. [http://dx.doi.org/10.1016/0022-5088\(81\)90154-5](http://dx.doi.org/10.1016/0022-5088(81)90154-5)
- [12] Pick, M., Davenport, J., Strogin, M. and Dienes, G. (1979) Enhancement of Hydrogen Uptake Rates for Nb and Ta by Thin Surface Overlayers. *Physical Review Letters*, **43**, 286-289. <http://dx.doi.org/10.1103/PhysRevLett.43.286>
- [13] Ares, J., Leardini, F., Díaz-Chao, P., Ferrer, I.J., Fernández, J.F. and Sánchez, C. (2014) Non-Isothermal Desorption Process of Hydrogenated Nanocrystalline Pd-Capped Mg Films Investigated by Ion Beam Techniques. *International Journal of Hydrogen Energy*, **39**, 2587-2596. <http://dx.doi.org/10.1016/j.ijhydene.2013.11.130>
- [14] Qu, J., Sun, B., Yang, R., Zhao, W., Wang, Y. and Li., X. (2010) Hydrogen Absorption Kinetics of Mg Thin Films under Mild Conditions. *Scripta Materialia*, **62**, 317-320. <http://dx.doi.org/10.1016/j.scriptamat.2009.11.033>
- [15] Johansson, M., Ostefeld, C. and Chorkkendorff, I. (2006) Adsorption of Hydrogen on Clean and Modified Magnesium Films. *Physical Review B*, **74**, Article ID: 193408. <http://dx.doi.org/10.1103/physrevb.74.193408>
- [16] Akyildiz, H., Özenbaş, M. and Öztürk, T. (2006) Hydrogen Absorption in Magnesium Based Thin Films. *International Journal of Hydrogen Energy*, **31**, 1379-1383. <http://dx.doi.org/10.1016/j.ijhydene.2005.11.003>
- [17] Mooij, L. and Dam, B. (2013) Nucleation and Growth Mechanisms of Nano Magnesium Hydride from the Hydrogen Sorption Kinetics. *Physical Chemistry Chemical Physics*, **15**, 11501-11510. <http://dx.doi.org/10.1039/c3cp51735g>
- [18] Kumar, S., Reddy, G. and Raju, V. (2009) Hydrogen Storage in Pd Capped Thermally Grown Mg Films: Studies by Nuclear Resonance Reaction Analysis. *Journal of Alloys and Compounds*, **476**, 500-506. <http://dx.doi.org/10.1016/j.jallcom.2008.09.080>
- [19] Olsson, S., Blomquist, P. and Hjärvarsson, B. (2001) Strain Dependant Phase Transitions of Hydrogen in Quasi-Two-Dimensional Vanadium Lattices. *Journal of Physics: Condensed Matter*, **13**, 1685-1698.
- [20] Andersson, G., Aits, K. and Hjärvarsson, B. (2002) Hydrogen Uptake of Thin Epitaxial Vanadium (001) Films. *Journal of Alloys and Compounds*, **334**, 14-19. [http://dx.doi.org/10.1016/S0925-8388\(01\)01743-1](http://dx.doi.org/10.1016/S0925-8388(01)01743-1)
- [21] Goncharov, A., Guglya, A. and Melnikova, E. (2012) On the Feasibility of Developing Hydrogen Storages Capable of Adsorption Hydrogen both in Its Molecular and Atomic States. *International Journal of Hydrogen Energy*, **37**, 18061-18073. <http://dx.doi.org/10.1016/j.ijhydene.2012.08.142>
- [22] Tal-Gutelmacher, E., Gemma, R., Pundt, A. and Kirchheim, R. (2010) Hydrogen Behavior in Nanocrystalline Titanium Thin Films. *Acta Materialia*, **58**, 3042-3049. <http://dx.doi.org/10.1016/j.actamat.2010.01.036>
- [23] Xiao, Z., Hauge, R. and Margrave, J. (1991) Reactions of Vanadium and Titanium with Molecular Hydrogen in Kr and Ar Matrices at 12K. *The Journal of Physical Chemistry*, **95**, 2696-2700. <http://dx.doi.org/10.1021/j100160a015>
- [24] Moehlecke, S., Majkrzak, C. and Strongin, M. (1985) Enhanced Hydrogen Solubility in Niobium Films. *Physical Review B*, **31**, 6804-6806. <http://dx.doi.org/10.1103/PhysRevB.31.6804>
- [25] Steiger, J., Blässer, S. and Weidinger, A. (1994) Solubility of Hydrogen in Thin Niobium Films. *Physical Review B*, **49**, 5570-5574. <http://dx.doi.org/10.1103/PhysRevB.49.5570>
- [26] Bouhtiyya, S. and Roué, L. (2008) On the Characteristic of Pd Thin Films Prepared by Pulsed Laser Deposition under Different Pressures. *International Journal of Hydrogen Energy*, **33**, 2912-2920. <http://dx.doi.org/10.1016/j.ijhydene.2008.04.013>

- [27] Lee, E., Lee, J.M., Koo, J.H., Lee, W. and Lee, T. (2010) Hysteresis Behavior of Electrical Resistance in Pd Thin Films during the Process of Absorption and Desorption of Hydrogen Gas. *International Journal of Hydrogen Energy*, **35**, 6984-6991. <http://dx.doi.org/10.1016/j.ijhydene.2010.04.051>
- [28] Özgüt, G., Akyıldız, H. and Öztürk, T. (2010) Isochronal Hydrogenation of Textured Mg/Pd Thin Films. *Thin Solid Films*, **518**, 4762-4767. <http://dx.doi.org/10.1016/j.tsf.2010.01.023>
- [29] Bouhtiyaa, S. and Roué, L. (2009) Pd/Mg/Pd Thin Films Prepared by Pulsed Laser Deposition under Different Helium Pressures: Structure and Electrochemical Hydriding Properties. *International Journal of Hydrogen Energy*, **34**, 5778-5784. <http://dx.doi.org/10.1016/j.ijhydene.2009.05.094>
- [30] Wirth, E., Munnik, F., Pranevičius, L. and Milcius, D. (2009) Dynamic Surface Barrier Effects on Hydrogen Storage Capacity in Mg-Ni Films. *Journal of Alloys and Compounds*, **475**, 917-922. <http://dx.doi.org/10.1016/j.jallcom.2008.08.036>
- [31] Qu, J., Wang, Y., Xie, L., Zheng, J., Liu, Y. and Li, X. (2009) Hydrogen Absorption-Desorption, Optical Transmission Properties and Annealing Effect of Mg Thin Films Prepared by Magnetron Sputtering. *International Journal of Hydrogen Energy*, **34**, 1910-1915. <http://dx.doi.org/10.1016/j.ijhydene.2008.12.039>
- [32] Norek, M., Stępniewski, W., Polański, M., Zasada, D., Bojar, Z. and Bystrzycki, J. (2011) A Comparative Study on the Hydrogen Absorption of Thin Films at Room Temperature Deposited on Non-Porous Glass Substrate and Nano-Porous Anodic Aluminum Oxide (AAO) Template. *International Journal of Hydrogen Energy*, **36**, 11777-11784. <http://dx.doi.org/10.1016/j.ijhydene.2011.06.046>
- [33] Reisfeld, R., Jisrawi, N., Ruckman, M. and Strongin, M. (1996) Hydrogen Absorption by Thin Pd/Nb Films Deposited on Glass. *Physical Review B*, **53**, 4974-4979. <http://dx.doi.org/10.1103/PhysRevB.53.4974>
- [34] Chung, C., Lee, S., Groves, J., Brower, E.N., Sinclair, R. and Clemens, B.M. (2012) Interfacial Alloy Hydride Establishment in Mg/Pd Thin Films. *Physical Review Letters*, **108**, Article ID: 106102. <http://dx.doi.org/10.1103/PhysRevLett.108.106102>
- [35] Guglya, A. (2005) Elektrofizicheskie i strukturno-fazovye kharakterisriki kompozitov Cr-N i V-N. *Vestnik Kharkovskogo Natsionalnogo Universiteta. Seriya: Yadra, tcastynki, polya*, **664**, 73-78. (In Russian)
- [36] Vasilenko, R., Goncharov, A., Guglya, A., et al. (2008) O mekhanizme formirovaniya V-N pokrytiy v usloviyah bombardirovki gazovimy ionami. *Poverhnost Rentgenovskie, Sinhrotronnie i Neytronnie Issledovaniya*, **11**, 81-87. (In Russian)
- [37] Bendikov, V., Guglya, A., Marchenko, I., Malykhin, D. and Neklyudov, I. (2003) Mechanisms of Forming the Cr-N Composite in the Unsteady-State Stage of Ion Beam-Assisted Deposition Process. *Vacuum*, **70**, 331-337. [http://dx.doi.org/10.1016/S0042-207X\(02\)00666-8](http://dx.doi.org/10.1016/S0042-207X(02)00666-8)
- [38] Takano, I., Isobe, S., Sasaki, T. and Baba, Y. (1989) High Nitrogen Ion-Implantation into Zirconium. *Applied Surface Science*, **37**, 25-32. [http://dx.doi.org/10.1016/0169-4332\(89\)90970-7](http://dx.doi.org/10.1016/0169-4332(89)90970-7)
- [39] Mansur, L. and Coghlan, W. (1983) Mechanisms of Helium Interaction with Radiation Effects in Metals and Alloys: A Review. *Journal of Nuclear Materials*, **119**, 1-25. [http://dx.doi.org/10.1016/0022-3115\(83\)90047-8](http://dx.doi.org/10.1016/0022-3115(83)90047-8)
- [40] Gladkih, N., Dukarov, S., Kryshtal, A., et al. (2004) Poverhnostnye yavleniya i fazovye prevrascheniya v kondensirovanyh plenkah. Kharkov. KNU im. V.N.Karasin.
- [41] Frenkel, I. (1924) Theorie der Adsorption und verwandter Erscheinungen. *Zeitschrift für Physik*, **26**, 117-138. <http://dx.doi.org/10.1007/BF01327320>
- [42] Belyakov, L., Makarova, T., Sakharov, V., Serenkov, I. and Sreseli, O. (1998) Sostav i poristost mnogokomponentnuh struktur: Poristiy kremniy kak trehkomponentnaya. *Fizika i Tekhnika Poluprovodnikov*, **32**, 1122-1124. [*Semiconductors*, **32**, 1003-1005].
- [43] Gringoz, A., Glandut, N. and Valette, S. (2009) Electrochemical Hydrogen Storage in TiC_{0.6}, Not in TiC_{0.9}. *Electrochemistry Communications*, **11**, 2044-2047. <http://dx.doi.org/10.1016/j.elecom.2009.08.049>
- [44] Ding, H., Fan, X., Li, C., Liu, X., Jiang, D. and Wang, C. (2013) First-Principles Study of Hydrogen Storage in Non-Stoichiometric TiC_x. *Journal of Alloys and Compounds*, **551**, 67-71. <http://dx.doi.org/10.1016/j.jallcom.2012.10.067>
- [45] Carbia, I., Lopez, M. and Alonso, J. (2007) The Optimum Average Nanopore Size Hydrogen Storage in Carbon Nanoporous Materials. *Carbon*, **45**, 2649-2658. <http://dx.doi.org/10.1016/j.carbon.2007.08.003>